Photochemical & Photobiological Sciences

Accepted Manuscript

This is an *Accepted Manuscript*, which has been through the Royal Society of Chemistry peer review process and has been accepted for publication.

Accepted Manuscripts are published online shortly after acceptance, before technical editing, formatting and proof reading. Using this free service, authors can make their results available to the community, in citable form, before we publish the edited article. We will replace this *Accepted Manuscript* with the edited and formatted *Advance Article* as soon as it is available.

You can find more information about *Accepted Manuscripts* in the Information for Authors.

Please note that technical editing may introduce minor changes to the text and/or graphics, which may alter content. The journal's standard Terms & Conditions and the Ethical guidelines still apply. In no event shall the Royal Society of Chemistry be held responsible for any errors or omissions in this *Accepted Manuscript* or any consequences arising from the use of any information it contains.

ROYAL SOCIETY OF CHEMISTRY

www.rsc.org/pps

Journal Name

RSCPublishing

ARTICLE

Singlet oxygen photosensitisation by the fluorescent protein Pp2FbFP L30M, a novel derivative of *Pseudomonas putida* flavin-binding Pp2FbFP†,‡

Cite this: DOI: 10.1039/x0xx00000x

Received 00th January 2012,
Accepted 00th January 2012

DOI: 10.1039/x0xx00000x

www.rsc.org/

Joaquim Torra,[a] Andrés Burgos-Caminal,[a] Stephan Endres,[b] Marcus Wingen,[b] Thomas Drepper,[b] Thomas Gensch,[c] Rubén Ruiz-González[a] and Santi Nonell*[a]

Flavin-binding fluorescent proteins (FbFPs) are a class of fluorescent reporters that are being increasingly used as reporters for the study of cellular structures and dynamics. Flavin's intrinsic high singlet oxygen ($^1O_2$) quantum yield (Φ_Δ = 0.51) provides a basis for the development of new FbFP mutants capable of photosensitising $^1O_2$ for mechanistic and therapeutic applications, as recently exemplified by the FbFP miniSOG. In the present work we report an investigation on $^1O_2$ photoproduction by Pp2FbFP L30M, a novel derivative of *Pseudomonas putida* Pp2FbFP. Direct detection of $^1O_2$ through its phosphorescence at 1275 nm yielded the value Φ_Δ = 0.09±0.01, which is the highest $^1O_2$ quantum yield reported to date for any FP and approximately 3-fold higher than the Φ_Δ for miniSOG. Unlike miniSOG, transient absorption measurements revealed the existence of two independent triplet states each with a different ability to sensitise $^1O_2$.

Introduction

The 2008 Chemistry Nobel Prize recognised the discovery, expression and development of the Green Fluorescent Protein (GFP).[1–3] GFP-like proteins have been extensively used to monitor and keep track of relevant biological processes.[4,5] Over the last fifteen years, increasing research efforts have been made to engineer new fluorescent proteins (FPs) with novel and/or enhanced properties. The diversity of currently available FPs covers nearly the entire visible spectrum, providing numerous alternative possibilities for multicolour labelling and studies of protein interaction.[3]

It was soon realised that FPs could be used for purposes other than reporting cellular events and could actually be engineered as genetically-encoded actuators for mechanistic (e.g., chromophore-assisted light inactivation of proteins, CALI)[6] or therapeutic (e.g., photodynamic therapy, PDT)[7] applications.

For PDT applications, the generation of reactive oxygen species (ROS), particularly singlet molecular oxygen ($^1O_2$), is regarded as a key event for triggering cell death. The details of $^1O_2$ photosensitisation by molecular dyes, referred to as photosensitisers (PSs) are well understood, as are their limitations.[8,9] Since the PS is commonly delivered from the cell exterior, so far it has been hard to separately study the contributions of external and internal damage, nor has it been possible to fully control the PS' location and thus the primary site of photodamage.

An alternative approach is the use of genetically-encoded PSs, delivered to the cell by means of a DNA fragment, which can be tailored to express the protein at pre-selected loci. This minimises problems such as PS solubility, biocompatibility and subcellular localisation, thereby offering unprecedented control on intracellular $^1O_2$ generation.

KillerRed, a member of the GFP family, was the first rationally-designed photosensitising FP.[10–12] It could be shown that its mechanism of action involves the generation of the superoxide radical anion ($O_2^{\bullet-}$).[13–15] Other members of the GFP family sensitise $^1O_2$ instead, however only to a modest extent due to both the restricted access of molecular oxygen to the protein's chromophore as well as to its poor photosensitising properties.[16–19]

Flavin-binding fluorescent proteins (FbFPs), derived from blue-light photoreceptors of the LOV (light, oxygen, voltage) family, have recently raised much interest as $^1O_2$ generators due to their smaller size as compared to GFPs and also to the good photosensitising properties of flavins. In addition, these FPs are less sensitive to pH and do not need oxygen for chromophore maturation.[20–22] MiniSOG, the first reported small monomeric LOV-based FP for $^1O_2$ generation, was developed by directed

evolution replacing, among others, the photoactive Cys426 of the original photoreceptor. This prevents the formation of a covalent bond with its chromophore flavin mononucleotide (FMN) upon blue-light excitation, which would detract from its photosensitisation ability.[23] MiniSOG, with $^1O_2$ quantum yield Φ_Δ = 0.03±0.01,[24,25] showed a stronger photosensitisation ability than any member of the GFP family reported so far. The discovery of miniSOG has opened new possibilities for electron microscopy (EM) as well as for optical detection and imaging of cellular processes,[23,26,27] contributing to the development of optogenetics.[28,29] Its potential for cell photokilling has now been confirmed[12,24,30,31] and mechanistic studies have revealed that it can generate not only $^1O_2$ but also $O_2^{\bullet-}$, as well as undergo electron-transfer (type-I) processes.[24,25]

The strategy followed to develop miniSOG has been adopted by other research groups aiming at enhancing the fluorescence or photostability of FbFPs.[20,21,32] Compilations of FbFPs from different organisms have recently been published.[33,34] A pre-screening of a number of such FbFPs in our laboratories for cell phototoxicity (data not shown) lead us to select the Pp2FbFP L30M mutant as a promising $^1O_2$ generator.

We report herein a full characterisation of its ability to photosensitise $^1O_2$ that reveal a number of important aspects that affect the properties and further development of this new class of photosensitising FbFPs.

Experimental Section

Chemicals

FMN was purchased from ChromaDex™ (Irvine, California) and used as received. Phosphate buffer solution (PBS) containing 10 mM NaCl, 10 mM NaH_2PO_4, pH 7.4 were prepared dissolving the required amount of a PBS tablet (Sigma) in milliQ water. In order to vary the concentration of oxygen in the solution, a stream of argon 5.0 or oxygen 5.0 (Carburos Metálicos) was flowed above the protein solution under gentle stirring for *ca.* 30 minutes.

Expression, purification and characterisation of Pp2FbFP L30M

Pp2FbFP L30M was obtained as reported by Wingen *et al.*[33] Basically, the *E. coli* strain DH5α was used for DNA cloning of the expression vectors encoding Pp2FbFP L30M. In turn, the *E. coli* strain BL21(DE3) (Novagen, distributed by Merck KGaA, Darmstadt, Germany) was used for expression. On basis of the already described fluorescent reporter protein Pp2FbFP,[20] the new variant Pp2FbFP L30M was constructed by the substitution of the amino acid residue leucine at position 30 by methionine. To achieve this, an overlap-extension polymerase chain reaction (PCR) was conducted using the flanking primer pair Pp2FbFP *NdeI* up: 5'-CATATGATCAACGCAAAACTCCTGC-3' and Pp2FbFP *XhoI* dn: 5'-CTCGAGTCAGTGCTTGGCCTGGCCCT-3'. The mutation was inserted into the coding sequence by using the primers Pp2FbFP L30M mut up: 5'-TGAGAGCATCATGATCTACGTCAAC-3' and Pp2FbFP L30M mut dn: 5'-GTTGACGTAGATCATGATGCTCTCA-3'. PCRs were performed using Phusion® High-Fidelity DNA polymerase (Thermo Scientific, Darmstadt, Germany) following the manufacture's guidelines. Subsequent the correct sequence of Pp2FbFP L30M was confirmed by DNA-sequencing. Prior to protein expression and purification, the Pp2FbFP L30M-encoding gene was cloned into the *NdeI* and *XhoI* restriction sites of pET28a (Novagen, distributed by Merck KGaA, Darmstadt, Germany) expression vector.

For gene expression and protein purification, bacterial cells were grown in 1 liter auto-induction terrific broth (TB) medium containing 12 g L^{-1} hydrolysed casein and 24 g L^{-1} yeast extract, 9.4 g L^{-1} K_2HPO_4, 2.2 g L^{-1} KH_2PO_4, (pH 7.2), 4 mL L^{-1} glycerol, 0.05% glucose, 0.2% lactose in 5 liter shake flasks at 37 °C for 24 hours. All media were supplemented with 50 µg mL^{-1} kanamycin to maintain the expression vectors. Pp2FbFP L30M was purified as His_6-tagged protein using Ni-NTA metal ion-exchange chromatography superflow columns (Qiagen, Hilden, Germany) under standard operation conditions as described by the manufacturer. The purified protein was stored at 4 °C in PBS buffer. Pp2FbFP L30M samples were always filtered through a 0.22 µm filter prior to their use. Detection and quantification of the flavin chromophores, i.e. FMN, FAD (flavin adenine dinucleotide), RF (riboflavin) and LC (lumichrome), respectively, were conducted as described previously.[35] A HPLC system from Shimadzu (LC10Ai; Shimadzu Deutschland, Duisburg, Germany) was used, employing a Select HSS T3 2.5 µm column (Waters GmbH, Eschborn, Germany). Pure flavins (FMN, FAD, and LC: Sigma-Aldrich, St. Louis, MO; RF: AppliChem GmbH, Darmstadt, Germany) were used as respective reference compounds.

Photophysical measurements

All photophysical measurements were carried out in PBS buffer at protein concentration of approximately 5 µM. Fresh samples from two different expression batches of Pp2FbFP L30M were used for each experiment. Results are the mean of at least three different independent determinations on each batch. Absorption and fluorescence spectra were recorded on a double beam Cary 6000i spectrophotometer (Varian) and a Spex Fluoromax-4 spectrofluorometer, respectively.

Time-resolved fluorescence and phosphorescence measurements were carried out using a customised PicoQuant Fluotime 200 fluorescence lifetime system and the FluoFit 5.0 software for data analysis. For fluorescence assays, excitation was achieved by means of a picosecond diode laser at 375 nm (PicoQuant, 10 MHz repetition rate, 50 ps pulsewidth) maintaining the counting frequency always below 1 %. For direct $^1O_2$ phosphorescence detection, the frequency-tripled output of a diode-pumped pulsed Nd:YAG laser (FTSS355-Q, Crystal Laser, Berlin, Germany) was used for excitation, working at 1 kHz repetition rate at 355nm (0.5 mW, or 0.5 µJ per puls, 1 ns pulsewidthe). A 1064 nm rugate notch filter (Edmund Optics, U.K.) was placed at the exit port of the laser

to remove any residual component of its fundamental emission in the NIR region. The luminescence exiting from the side of the sample was filtered by two long-pass filters of 355 and 532 nm (Edmund Optics, U.K.) and two narrow bandpass filters at 1275 nm (NB-1270-010, Spectrogon, Sweden and bk-1270-70-B, bk Interfernzoptik, Germany) to remove any scattered laser radiation and isolate the $^1O_2$ emission. A TE-cooled Hamamatsu NIR sensitive photomultiplier tube assembly (H9170-45, Hamamatsu) was used as detector. Photon counting was achieved with a multichannel scaler (PicoQuant's Nanoharp 250).

Transient absorption experiments in the UV-Vis region were carried out using a home-built nanosecond laser flash photolysis system. In this instrument, the 3rd harmonic (355 nm) of a Continuum Surelite I-10 Nd:YAG laser (5 ns pulse width, 7.5 mJ per pulse) was directed to the sample. Changes in the sample absorbance were detected at 700 nm using a Hamamatsu R928 photomultiplier to monitor the intensity variations of an analysis beam produced by a 75 W short arc Xe lamp (USHIO) and spectral discrimination was obtained using a PTI 101 monochromator. The signal was fed to a Lecroy Wavesurfer 454 oscilloscope for digitising and averaging (4 shots) and finally transferred to a PC for data storage and analysis. The TTL sync output of the laser was used to trigger the oscilloscope. The energy of the laser pulse was varied by neutral density filters and measured with a pyroelectric energy meter (RJP 735 and RJ 7610) from Laser Precision Corp. The system was controlled by the in house-developed LKS software (LabView, National Instruments).

All spectroscopic measurements were carried out using quartz cuvettes (Hellma) under magnetic stirring and at room temperature.

Fluorescence quantum yields (Φ_F) were determined by comparing the area under the fluorescence curve (AUC) for optically matched solutions of sample and FMN as standard ($\Phi_{F,FMN} = 0.25$)[33] in the same solvent (PBS). The absorbance of sample and reference solutions was checked to be below 0.1 at the excitation wavelength to prevent inner filter effects.

The rate constant for oxygen quenching of the triplet state of Pp2FbFP L30M ($k_q^{O_2}$) was determined by measuring the lifetime of the triplet–triplet transient-absorption signals as a function of oxygen concentration in solution. Samples were excited at 355 nm and the resulting transients observed at 700 nm. A plot of the reciprocal lifetime vs oxygen concentration afforded $k_q^{O_2}$ as the slope of the linear fit. The concentration of molecular oxygen in the solutions was changed by gentle bubbling with solvent-saturated argon or oxygen for at least 30 min. The proportion of triplets quenched by oxygen, $P_T^{O_2}$, was calculated from $k_q^{O_2}$ and the intrinsic rate constant for triplet decay (k_T^0) according to eqn (1):

$$P_T^{O_2} = \frac{k_q^{O_2}[O_2]}{k_T^0 + k_q^{O_2}[O_2]} \quad (1)$$

The quantum yield of triplet formation (Φ_T) was determined by comparison of the zero-time transient-absorption amplitudes, $\Delta Abs(0)$, of optically matched solution96s of FMN ($\Phi_T = 0.6$)[36] and Pp2FbFP L30M, according to eqn (2), assuming approximately equal triplet absorption coefficients at the observation wavelength (700 nm).

$$\Phi_T(\text{Pp2FbFP L30M}) = \Phi_T(\text{FMN}) \frac{\Delta Abs(0)_{\text{Pp2FbFP L30M}}}{\Delta Abs(0)_{\text{FMN}}} \quad (2)$$

The procedure for the determination of Φ_Δ is described in detail in the Discussion section.

Results

Absorption and fluorescence properties of Pp2FbFP L30M

HPLC analysis of the chromophore composition of Pp2FbFP L30M revealed approximately equal amounts of FMN (46%) and FAD (41%) as the main chromophores, as well as minor amounts of (LC, 11%) and RF (2%).

Absorption and emission spectra for Pp2FbFP L30M and reference FMN are shown in Fig. 1. The absorption spectrum of FMN has only two maxima with a shoulder in the longest-wavelength part of the spectrum, while Pp2FbFP L30M shows three bands in the blue and two bands in the near-UV spectral range. The same trend is true for the fluorescence, where the spectrum of FMN is featureless and about 30 nm red-shifted compared to the two-band spectrum of Pp2FbFP L30M.

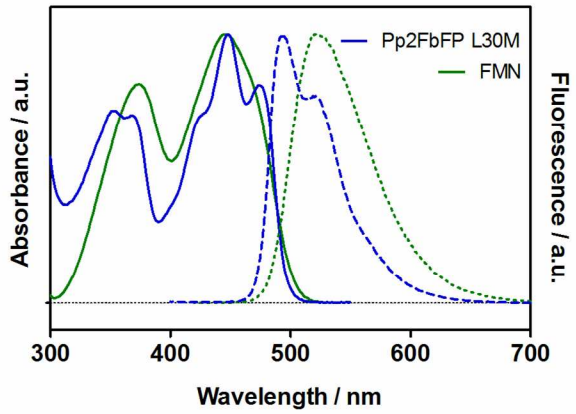

Fig. 1 Normalised absorption (solid lines) and emission (dashed lines) spectra of Pp2FbFP L30M (blue) and FMN (green). λ_{exc} = 355 nm

The fluorescence quantum yield of Pp2FbFP L30M is Φ_F = 0.25±0.01, which is close to the value reported for free FMN in solution[32] but substantially smaller than that of miniSOG (Φ_F = 0.41 ± 0.01).[33] Time resolved emission spectroscopy (TRES) revealed the presence of two components with almost identical spectrum but different lifetimes, 3.5 ns and 5.2 ns respectively, and different relative amplitudes (70% and 30%; Fig. 2).

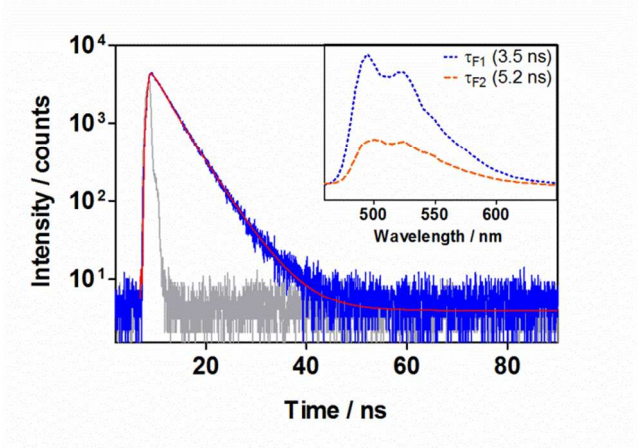

Fig. 2 Fluorescence decay of Pp2FbFP L30M (blue trace), fitted function (red line) and instrument response function (grey trace). λ_{exc} = 375 nm and λ_{obs} = 500 nm. Inset: TRES spectra of the fast (dotted line) and slow (dashed line) components.

Singlet-oxygen production yield and kinetics.

Production of $^1O_2$ by Pp2FbFP L30M was assessed by observation of its phosphorescence at 1275 nm[37] (Fig. 3).

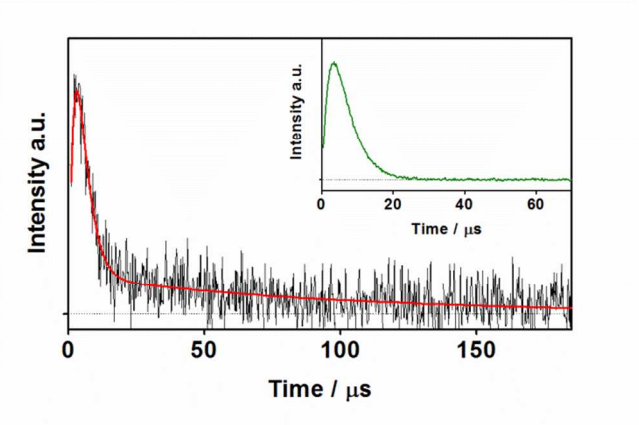

Fig. 3 Time-resolved $^1O_2$ phosphorescence for Pp2FbFP L30M in air-saturated PBS solution. The corresponding trace for FMN is shown in the inset for comparison; notice the absence of the long-lived tail. Fitted function in red. λ_{exc} = 355 nm; λ_{obs} = 1275 nm

Three exponentials were needed to adequately fit the data: one component for the growth (negative amplitude) and two components for the decay (positive amplitudes, see eqn (3)). In contrast, the signals for the reference FMN could be fitted by just one growth and one decay components, as is usually found for molecular PSs in homogeneous sytems.[38]

$$S_t = -A_1 e^{-t/\tau_1} + A_2 e^{-t/\tau_2} + A_3 e^{-t/\tau_3} \qquad (3)$$

With this notation, the three coefficients $A_{1\text{-}3}$ are all positive. The time constants of the rise and longest-decay components were affected by oxygen, while that for the shortest decay remained unaltered (Table 1). Moreover, the intensity of the signal increased substantially upon oxygen saturation (Figure S1 in the ESI).

Table 1. Time constants of the $^1O_2$ growth and decay kinetics in air-saturated PBS solutions. Values in parentheses correspond to oxygen-saturated solutions. The uncertainties are ± 0.2 μs.

	τ_1 / μs[a]	τ_2 / μs[b]	τ_3 / μs[b]
Pp2FbFP L30M	2.6 (0.9)	3.3	84 (65)
FMN	2.7 (0.7)	3.8	-

[a] growth, [b] decay

Triplet-state kinetics

The flavin's triplet state was probed by transient absorption spectroscopy at 700 nm. Similarly as in the fluorescence experiments, the signals in argon-saturated solutions also showed two exponential components with similar amplitudes though different lifetimes (Fig. 4). Both could be quenched by oxygen, albeit with different rate constants (Table 2 and Fig S2 in the ESI), and the decay rate constants in air- and oxygen-saturated solutions matched those derived from $^1O_2$ phosphorescence experiments, confirming their assignment to triplet states. Exposure to oxygen caused additionally the decrease in the signal amplitude for the short-lived component. Comparison of the zero-time amplitude to that of free FMN (eqn (2)) yielded the triplet quantum yield value of Φ_T = 0.30 ± 0.06 in argon-saturated solutions (Fig. S3 in the ESI).

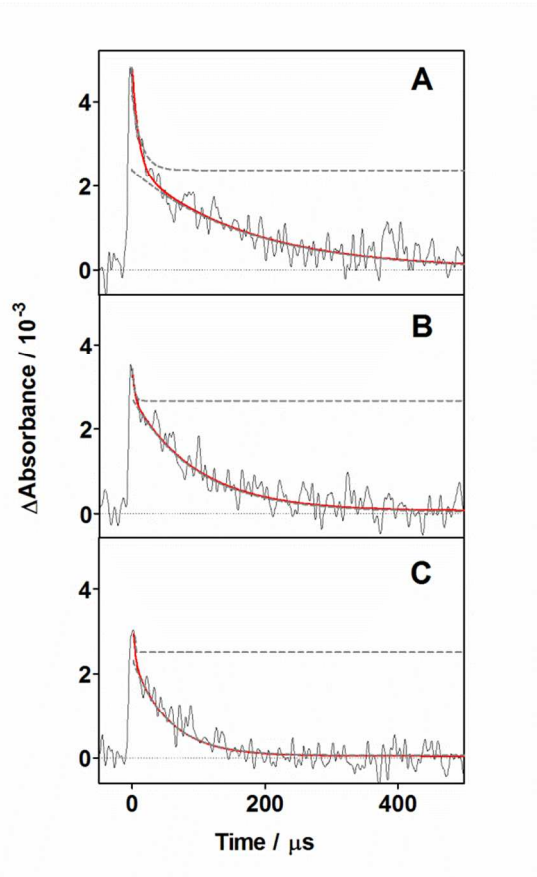

Fig. 4 Transient absorption decays for Pp2FbFP L30M in (A) argon, (B) air and (C) oxygen-saturated solutions. The overall fit (solid line) and individual decay components (dashed lines) are shown for comparison of their relative

contribution to the overall signal. Transients are the average of 4 shots. λ_{exc} = 355 nm and λ_{obs} = 700 nm.

Table 2. Summary of triplet excited state kinetics for sample and reference.

	τ_T / µs [a]	$k_q^{O_2}$ / 10^9 $M^{-1}s^{-1}$	$P_T^{O_2}$ [b]
Pp2FbFP L30M	18 (45%)	1.9 ± 0.2	0.83 (0.96)
	154 (55%)	0.0086 ± 0.002	0.22 (0.59)
FMN	42 (100%)	1.0 ± 0.2 [39]	0.91 (0.98)

[a] Uncertainty 10%. Fractional amplitudes in parentheses, [b] Uncertainty 10%. Proportion of triplets trapped by molecular oxygen in air-saturated solutions (values in parentheses correspond to oxygen-saturated solutions).

Discussion

Flavin binding by Pp2FbFP L30M

HPLC analysis of the chromophores in Pp2FbFP L30M reveals that it binds FMN and FAD to similar extents, along with small amounts of RF and LC (Figure S5B in the ESI). This contrasts with miniSOG, which almost exclusively binds FMN (Figure S5C in the ESI).[23] Since FMN and FAD are both natural components of cells, this heterogeneous binding is probably unavoidable. It is worth noting that absolute and relative concentrations of the different flavins are variable both between different cell types as well as temporally within one cell type depending on the respective LOV protein, the used expression system as well as the storage conditions after purification as observed previously.[35,40,41] Attempts to characterize the influence of each individual flavin species bound to the FbFP on the photophysical properties of the protein are currently in progress.

Photophysics of Pp2FbFP L30M

The absorption and fluorescence spectra of Pp2FbFP L30M depict the same features observed in typical FbFPs: blue-shifts with respect to free FMN and well-resolved vibronic structure. This indicates that the flavins are confined within the protein active pocket, where their mobility is much restricted.[42] Likewise, the Stokes shift between the emission and absorption spectra is smaller than for FMN, indicating a smaller change in dipole moment upon excitation, again consistent with protein binding. Compared to Pp2FbFP, the effects of the L30M mutation on the photophysics are minor, namely a small 1-nm blue shift in the spectra and a slight increase in the Φ_F value (0.25 vs 0.22).[33]

Regarding the time course of the fluorescence, Pp2FbFP L30M shows a biexponential decay with the two components showing a similar spectrum, which matches the observations for the parent protein and previously-described variants.[33] However there is a substantial difference between the two proteins, namely the longer lifetime of the second component (5.2 vs 0.93 ns) while the first one is essentially unchanged (3.5 vs. 3.6 ns). In the parent protein, the short lifetime has been attributed to the efficient quenching of the FMN fluorescence by nearby amino acids.[33] Either such dynamic quenching would be of much lesser important in the L30M mutant or the 5.2 ns components is due to a different flavin. All in all, the results above, together with the transient absorption and $^1O_2$ data, are in line with the existence of at least two different flavins in the protein samples, although contributions of different protein conformers and/or the formation of protein dimers[33] cannot be excluded at present.

Triplet-state properties and oxygen accessibility to the chromophore

In agreement with the fluorescence results, transient absorption also confirms a dual population of triplet flavins in Pp2FbFP L30M, each with its own lifetime. The observed Φ_T value is roughly half of that for free FMN and is in line with the reported values for LOV domains, which range from 0.25 to 0.65.[43–46] Also, the Φ_T value is close to that of miniSOG.[24]

Since oxygen quenching of triplet states is a diffusion-controlled process, it provides information on the accessibility of oxygen to the flavin within the protein. The $k_q^{O_2}$ value for the short-lived triplet is similar to that of free FMN, which indicates a very exposed flavin, as in miniSOG.[24] This allows for an efficient trapping by molecular oxygen (Table 2). In contrast, the long-lived triplet is far less accessible to molecular oxygen and the trapping efficiency is much lower (Table 2). The marked differences among the two triplets anticipate distinct contributions to their respective $^1O_2$ photosensitisation ability.

Assessing the $^1O_2$ quantum yield of Pp2L30M

Direct detection of $^1O_2$ by means of its phosphorescence at 1275 nm provides the most robust and specific method to quantify the production of this reactive species. In a previous communication we compared this technique with two chemical trapping methods for the related FbFP miniSOG.[24] Our results revealed the limitations of the chemical acceptor anthracene dipropionate (ADPA) used in ref. 23, shown to be oxidized also by non-singlet oxygen pathways, and established the validity of the near-IR phosphorescence approach. It is reassuring that our results were independently reproduced by another laboratory.[25]

The phosphorescence of $^1O_2$, S_t, is proportional to the concentration of this ROS. In homogeneous environments, S_t typically shows a rise-and-decay profile, as given by eqn (4),[38] arising from the formation and deactivation of $^1O_2$ in the medium.

$$S_t = S_0 \frac{\tau_\Delta}{\tau_\Delta - \tau_T}\left(e^{-\frac{t}{\tau_\Delta}} - e^{-\frac{t}{\tau_T}}\right) \quad (4)$$

The empirical parameter S_0 is proportional to Φ_Δ and is therefore used to assess the ability of a given PS to produce $^1O_2$ by comparing its $S(0)$ value to that of a reference PS measured under the same experimental conditions (eqn (5)).[38]

$$\Phi_\Delta(\text{sample}) = \Phi_\Delta\ (\text{ref}) \times \frac{S_0(\text{sample})}{S_0\ (\text{ref})} \quad (5)$$

However, in heterogeneous systems such as biological media the signal no longer obeys eqn (4) and more complex rate laws are required to fit the data. Several kinetic models have been proposed over the years for $^1O_2$ formation in such systems.[38,47,48] In connection with chromophores embedded into

a protein matrix, Lepeshkevich *et al.* have recently proposed a model that distinguishes between $^1O_2$ populations inside and outside the protein.[49] The mathematical solution to the differential equations proposed in this model leads to a triexponential function, as shown in eqn (6).

$$S_t = \chi_1 e^{-\alpha_1 t} - \chi_2 e^{-\alpha_2 t} + (\chi_2 - \chi_1) e^{-\alpha_3 t} \quad (6)$$

Despite the formal similarity of eqn (6) to the empirically-determined eqn (3), the constraints in the χ_i preexponential factors in eqn (6) made it impossible to fit this model to our data. This was actually to be expected since Lepeshkevich *et al.*'s model assumes a single population of triplet states, a condition that does not hold in our protein samples. The simplest alternative model considers two independent flavins, each producing $^1O_2$ with its own set of kinetics and yields (Scheme 1).

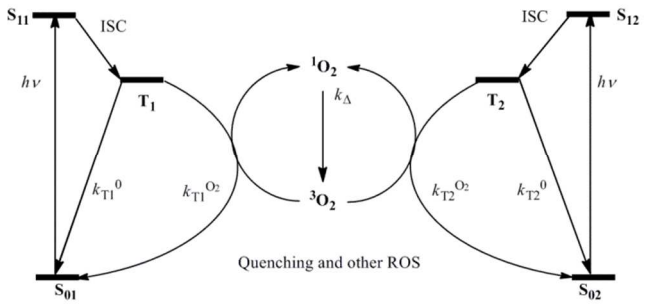

Scheme 1 Kinetic model of $^1O_2$ generation from two independent triplet excited states. See text for details.

A few ns after the laser pulse the initial triplet concentrations $[T_1]_0$ and $[T_2]_0$ are formed. In the absence of oxygen, the triplets decay back to the ground state with a rate constant k_T^0. If oxygen is allowed into the system, additional decay channels arise for the triplet, in which it is quenched by oxygen to produce $^1O_2$ (and perhaps other ROS). Finally, $^1O_2$ deactivates with a rate constant k_Δ. Alternative processes such as $^1O_2$ diffusion within the protein are not considered because there is no evidence for such processes in our luminescence data (see Fig. 3 and eqn (3)). Thus, the concentration of $^1O_2$ can be described by eqn (7):

$$[^1O_2] = I_{abs}\frac{A_1}{A_1+A_2}\Phi_{\Delta_1}\frac{k_{T_1}}{k_{T_1}-k_\Delta}\left(e^{-k_\Delta t} - e^{-k_{T_1} t}\right) + I_{abs}\frac{A_2}{A_1+A_2}\Phi_{\Delta_2}\frac{k_{T_2}}{k_{T_2}-k_\Delta}\left(e^{-k_\Delta t} - e^{-k_{T_2} t}\right), \quad (7)$$

where I_{abs} is the amount of light absorbed per unit volume and A_i is the absorbance of flavin *i* at the excitation wavelength.

Since the phosphorescence of $^1O_2$ is proportional to the concentration of $^1O_2$, eqn (7) can be rewritten as eqn (8):

$$S_t = S_{01}\frac{\tau_\Delta}{\tau_\Delta-\tau_{T_1}}\left(e^{-\frac{t}{\tau_\Delta}} - e^{-\frac{t}{\tau_{T_1}}}\right) + S_{02}\frac{\tau_\Delta}{\tau_\Delta-\tau_{T_2}}\left(e^{-\frac{t}{\tau_\Delta}} - e^{-\frac{t}{\tau_{T_2}}}\right) \quad (8)$$

which fits well the data (see eqn (3)), thus yielding S_{01} and S_{02}. The Φ_Δ value for the Pp2FbFP L30M protein can then be determined using eqn (9):

$$\Phi_\Delta = \Phi_\Delta^{st}\frac{S_{01}+S_{02}}{S_0^{st}} \quad (9)$$

Eqn (9) relies on the assumption that the radiative rate constant of the two populations of $^1O_2$ are similar, which is likely the case as we observe one single decay for all $^1O_2$ molecules, meaning a similar environment. Taking FMN as standard (Φ_Δ = 0.51)[39], eqn (9) yielded a Φ_Δ value of 0.09 ± 0.01 for Pp2FbFP L30M, which is the highest value reported to date for a genetically encoded PS.

The individual S_{01} and S_{02} values (Fig. S4 in the ESI) indicate that 30% of the protein $^1O_2$ signal arises from the short-lived, oxygen-accessible triplet, whereas 70% arises from the long-lived, less-accessible one, despite the oxygen trapping efficiencies being the opposite (Table 2). This would indicate that the triplet quantum yield is larger for the longest-lived triplet, in agreement with the transient absorption results (Fig. 4). Despite its higher complexity, Pp2FbFP L30M outperforms miniSOG in terms of $^1O_2$ photosensitisation by a factor of approximately 3. A structural interpretation of the enhanced photosensitisation ability is unfortunately not possible at present since the protein structures of miniSOG and Pp2FbFP are not solved so far. However, the sequence alignment (Figure S6 in the ESI) clearly demonstrates that the methionine at position 30 of the presented Pp2FbFP variant is not conserved in other selected LOV-derived florescent proteins including miniSOG: With exception of DsFbFP,[33] all of the shown LOV-based FPs harbour either an isoleucine or a leucine residue at the corresponding position. Furthermore, four of the five residues of miniSOG that have been changed in the original LOV2 domain of *A. thaliana* phototropin 2 (At Phot2) to yield higher $^1O_2$ production rates (position 1-4 in the alignment) cannot be found in Pp2FbFP L30M. Thus, the low sequence homology (the sequence identity of Pp2FbFP L30M and miniSOG is 27%) suggests that the increased $^1O_2$ quantum yields of Pp2FbFP L30M and miniSOG are caused by different, so far uncharacterized structural effects.

Conclusions

Pp2FbFP L30M has been engineered building upon previous knowledge of the effect of the L30 position on the photochemical behaviour of LOV photoreceptors.[50,51] Pp2FbFP L30M has been demonstrated to photosensitise $^1O_2$ upon light irradiation through detection of its phosphorescence at 1275 nm. Its $^1O_2$ quantum yield (Φ_Δ= 0.09±0.01) is the highest reported to date for any genetically-encoded PS, which makes it a very promising candidate for biological applications such as CALI or PDT. Of specific interest, FbFPs can now be expressed at pre-defined subcellular sites, thus offering unprecedented spatiotemporal control of ROS generation.[30] Time-resolved absorption and fluorescence indicate that Pp2FbFP L30M generates two different triplet excited states

with an overall quantum yield of approximately $\Phi_T = 0.3$. Both triplets are capable of sensitising $^1O_2$ but show different degrees of oxygen accessibility. These observations likely reflect the distribution of different flavin chromophores in the protein samples; however, other possibilities such as a dynamic protein conformation equilibrium or, less likely, the formation of asymmetric protein dimers, could also contribute for this outcome.

Overall, we have shed light on the photochemical behaviour of Pp2FbFP L30M derivative by means of a wide range of spectroscopic techniques. Our findings are likely to contribute to the development of more efficient LOV-based $^1O_2$ sensitising FbFPs that can achieve values of Φ_Δ closer to that of the free FMN prosthetic group ($\Phi_\Delta = 0.51$). They also highlight the complications one may encounter in the characterisation of the photosensitising properties of LOV-based FPs.

Acknowledgements

Financial support for this research was obtained from the Spanish Ministry of Economy and Competitivity (CTQ2013-48767-C3-1-R). We further thank the Ministry of Innovation, Science and Research of North Rhine-Westphalia and Heinrich-Heine-University Düsseldorf for the scholarship within the CLIB-Graduate Cluster Industrial Biotechnology and funding by the NRW-Strategieprojekt BioSC. The authors would also like to thank Astrid Wirtz (University of Düsseldorf) for the chromatographic analysis of Pp2FbFP L30M flavin chromophores.

Notes and references

[a] Institut Químic de Sarrià, Universitat Ramon Llull, Via Augusta 390, 08017, Barcelona, Spain.
[b] Institute of Molecular Enzyme Technology, Heinrich-Heine-University Düsseldorf, Forschungszentrum Jülich, 52425 Jülich, Germany.
[c] Institute of Complex Systems 4 (ICS-4, Cellular Biophysics), Forschungszentrum Jülich, 52425 Jülich, Germany.

† Electronic Supplementary Information (ESI) available: Pp2FbFP L30M $^1O_2$ phosphorescence kinetics. Effect of oxygen concentration on the rate of Pp2FbFP L30M triplet state decay. Transient absorbance decays. Deconvolution of $^1O_2$ phosphorescence

‡ Dedicated to Professor Kristian Berg on the occasion of his 60th birthday.

. See DOI: 10.1039/b000000x/

1. O. Shimomura, *Methods Biochem. Anal.*, 2008, **47**, 1–13.
2. M. Chalfie, *Proc. Natl. Acad. Sci. U. S. A.*, 2008, **106**, 10073–10080.
3. R. Y. Tsien, *Angew. Chemie Int. Ed.*, 2009, **48**, 5612–5626.
4. R. N. Day and M. W. Davidson, *Chem. Soc. Rev.*, 2009, **38**, 2887–2921.
5. D. M. Chudakov, M. V Matz, S. Lukyanov, and K. A. Lukyanov, *Physiol Rev*, 2010, **90**, 1103–1163.
6. T. Surrey, M. B. Elowitz, P. E. Wolf, F. Yang, F. Nedelec, K. Shokat, and S. Leibler, *Proc. Natl. Acad. Sci. U. S. A.*, 1998, **95**, 4293–4298.
7. L. Greenbaum, C. Rothmann, R. Lavie, and Z. Malik, *Biol. Chem.*, 2000, **381**, 1251–1258.
8. C. Schweitzer and R. Schmidt, *Chem. Rev.*, 2003, **103**, 1685–1758.
9. P. R. Ogilby, *Photochem. Photobiol. Sci.*, 2010, **9**, 1543– 1560.
10. M. E. Bulina, D. M. Chudakov, O. V Britanova, Y. G. Yanushevich, D. B. Staroverov, T. V Chepurnykh, E. M. Merzlyak, M. A. Shkrob, S. Lukyanov, and K. A. Lukyanov, *Nat. Biotechnol.*, 2006, **24**, 95–99.
11. J. Kobayashi, H. Shidara, Y. Morisawa, M. Kawakami, Y. Tanahashi, K. Hotta, and K. Oka, *Neurosci. Lett.*, 2013, **548**, 261–264.
12. M. V Shirmanova, E. O. Serebrovskaya, K. A. Lukyanov, L. B. Snopova, M. A. Sirotkina, N. N. Prodanetz, M. L. Bugrova, E. A. Minakova, I. V Turchin, V. A. Kamensky, S. A. Lukyanov, and E. V Zagaynova, *J. Biophotonics*, 2013, **6**, 283–290.
13. S. Pletnev, N. G. Gurskaya, N. V Pletneva, K. A. Lukyanov, D. M. Chudakov, V. I. Martynov, V. O. Popov, M. V Kovalchuk, A. Wlodawer, Z. Dauter, and V. Pletnev, *J. Biol. Chem.*, 2009, **284**, 32028–32039.
14. E. O. Serebrovskaya, E. F. Edelweiss, O. A. Stremovskiy, K. A. Lukyanov, D. M. Chudakov, and S. M. Deyev, *Proc. Natl. Acad. Sci. U. S. A.*, 2009, **106**, 9221–5.
15. R. B. Vegh, K. M. Solntsev, M. K. Kuimova, S. Cho, Y. Liang, B. L. W. Loo, L. M. Tolbert, and A. S. Bommarius, *Chem. Commun.*, 2011, **47**, 4887–4889.
16. A. Jiménez-Banzo, S. Nonell, J. Hofkens, and C. Flors, *Biophys. J.*, 2008, **94**, 168–172.
17. A. Jiménez-Banzo, X. Ragàs, S. Abbruzzetti, C. Viappiani, B. Campanini, C. Flors, and S. Nonell, *Photochem. Photobiol. Sci.*, 2010, **9**, 1336–1341.
18. R. Ruiz-González, J. H. White, M. Agut, S. Nonell, and C. Flors, *Photochem. Photobiol. Sci.*, 2012, **11**, 1411–1413.
19. K. Takemoto, T. Matsuda, N. Sakai, D. Fu, M. Noda, S. Uchiyama, I. Kotera, Y. Arai, M. Horiuchi, K. Fukui, T. Ayabe, F. Inagaki, H. Suzuki, and T. Nagai, *Sci. Rep.*, 2013, **3**, 2629.
20. T. Drepper, T. Eggert, F. Circolone, A. Heck, U. Krauss, J. K. Guterl, M. Wendorff, A. Losi, W. Gartner, and K. E. Jaeger, *Nat. Biotechnol.*, 2007, **25**, 443–445.
21. J. M. Christie, J. Gawthorne, G. Young, N. J. Fraser, and A. J. Roe, *Mol. Plant*, 2012, **5**, 533–544.
22. T. Drepper, T. Gensch, and M. Pohl, *Photochem. Photobiol. Sci.*, 2013, **12**, 1125–1134.
23. X. Shu, V. Lev-Ram, T. J. Deerinck, Y. Qi, E. B. Ramko, M. W. Davidson, Y. Jin, M. H. Ellisman, and R. Y. Tsien, *PLoS Biol.*, 2011, **9**, e1001041.
24. R. Ruiz-González, A. L. Cortajarena, S. H. Mejias, M. Agut, S. Nonell, and C. Flors, *J. Am. Chem. Soc.*, 2013, **135**, 9564–7.
25. F. M. Pimenta, R. L. Jensen, T. Breitenbach, M. Etzerodt, and P. R. Ogilby, *Photochem. Photobiol.*, 2013, **89**, 1116–1126.
26. D. Boassa, M. L. Berlanga, M. A. Yang, M. Terada, J. Hu, E. A. Bushong, M. Hwang, E. Masliah, J. M. George, and M. H. Ellisman, *J. Neurosci.*, 2013, **33**, 2605–2615.
27. E. M. Wurtzler and D. Wendell, *Biomacromolecules*, 2014, **15**, 228–233.
28. Y. B. Qi, E. J. Garren, X. Shu, R. Y. Tsien, and Y. Jin, *Proc. Natl. Acad. Sci. U. S. A.*, 2012, **109**, 7499–7504.

29. J. Y. Lin, S. B. Sann, K. Zhou, S. Nabavi, C. D. Proulx, R. Malinow, Y. Jin, and R. Y. Tsien, *Neuron*, 2013, **79**, 241–253.
30. A. P. Ryumina, E. O. Serebrovskaya, M. V Shirmanova, L. B. Snopova, M. M. Kuznetsova, I. V Turchin, N. I. Ignatova, N. V Klementieva, A. F. Fradkov, B. E. Shakhov, E. V Zagaynova, K. A. Lukyanov, and S. A. Lukyanov, *Biochim. Biophys. Acta*, 2013, **1830**, 5059–5067.
31. K. E. Mironova, G. M. Proshkina, A. V. Ryabova, O. A. Stremovskiy, S. A. Lukyanov, R. V. Petrov, and S. M. Deyev, *Theranostics*, 2013, **3**, 831–840.
32. S. Chapman, C. Faulkner, E. Kaiserli, C. Garcia-Mata, E. I. Savenkov, A. G. Roberts, K. J. Oparka, and J. M. Christie, *Proc. Natl. Acad. Sci. U. S. A.*, 2008, **105**, 20038–20043.
33. M. Wingen, J. Potzkei, S. Endres, G. Casini, C. Rupprecht, C. Fahlke, U. Krauss, K.-E. Jaeger, T. Drepper, and T. Gensch, *Photochem. Photobiol. Sci.*, 2014, **13**, 875–883.
34. A. Mukherjee, J. Walker, K. B. Weyant, and C. M. Schroeder, *PLoS One*, 2013, **8**, e64753.
35. Z. Cao, V. Buttani, A. Losi, and W. Gärtner, *Biophys. J.*, 2008, **94**, 897–905.
36. A. Losi, E. Polverini, B. Quest, and W. Gärtner, *Biophys. J.*, 2002, **82**, 2627–34.
37. A. Jiménez-Banzo, X. Ragàs, P. Kapusta, and S. Nonell, *Photochem. Photobiol. Sci.*, 2008, **7**, 1003–1010.
38. S. Nonell and S. E. Braslavsky, *Methods Enzymol.*, 2000, **319**, 37–49.
39. J. Baier, T. Maisch, M. Maier, E. Engel, M. Landthaler, and W. Bäumler, *Biophys. J.*, 2006, **91**, 1452–1459.
40. C. Schwerdtfeger and H. Linden, *EMBO J.*, 2003, **22**, 4846–55.
41. M. Dorn, M. Jurk, A. Wartenberg, A. Hahn, and P. Schmieder, *PLoS One*, 2013, **8**, e81268.
42. T. Schüttrigkeit, C. K. Kompa, M. Salomon, W. Rüdiger, and M. E. Michel-Beyerle, *Struct. Photosynth.*, 2003, **294**, 501–508.
43. U. Krauss, A. Losi, W. Gärtner, K.-E. Jaeger, and T. Eggert, *Phys. Chem. Chem. Phys.*, 2005, **7**, 2804–2811.
44. A. Losi, B. Quest, and W. Gärtner, *Photochem. Photobiol. Sci.*, 2003, **2**, 759–766.
45. A. Losi, T. Kottke, and P. Hegemann, *Biophys. J.*, 2004, **86**, 1051–1060.
46. S. D. M. Islam, A. Penzkofer, and P. Hegemann, *Chem. Phys.*, 2003, **291**, 97–114.
47. Y. Fu and J. R. Kanofsky, *Photochem. Photobiol.*, 1995, **62**, 692–702.
48. Y. Fu, P. D. Sima, and J. R. Kanofsky, *Photochem. Photobiol.*, 1996, **63**, 468–476.
49. S. V. Lepeshkevich, M. V. Parkhats, A. S. Stasheuski, V. V. Britikov, E. S. Jarnikova, S. A. Usanov, and B. M. Dzhagarov, *J. Phys. Chem. A*, 2014, **118**, 1864–1878.
50. J. M. Christie, S. B. Corchnoy, T. E. Swartz, M. Hokenson, I. S. Han, W. R. Briggs, and R. A. Bogomolni. *Biochemistry* 2007, **46**, 9310-9319.
51. B. D. Zoltowski, B. Vaccaro, and B. R. Crane, (2009). *Nat. Chem. Biol.* 2009, **5**, 827-834.